AD/A-002 124

PHYSICAL MODELS OF FIRES AND THEIR ASSOCIATED ENVIRONMENT

Andrew M. Stein, et al

RAND Corporation

Prepared for:

Pacific Southwest Forest and Range Experiment Station
California University

July 1973

DISTRIBUTED BY:

NTIS
National Technical Information Service
U. S. DEPARTMENT OF COMMERCE

PHYSICAL MODELS OF FIRES AND THEIR ASSOCIATED ENVIRONMENT

Andrew M. Stein

John G. Sullivan

Francis W. Murray

July 1973

P-5049

The Rand Paper Series

Papers are issued by The Rand Corporation as a service to its professional staff. Their purpose is to facilitate the exchange of ideas among those who share the author's research interests; Papers are not reports prepared in fulfillment of Rand's contracts or grants. Views expressed in a Paper are the author's own, and are not necessarily shared by Rand or its research sponsors.

The Rand Corporation
Santa Monica, California 90406

PHYSICAL MODELS OF FIRES AND THEIR ASSOCIATED ENVIRONMENT*

Andrew M. Stein, Research Physicist
Fire Research Laboratory, Pacific Southwest Forest and
Range Experiment Station, Riverside, California

John G. Sullivan, Systems Analyst-Programmer
University of California, Riverside, California

Francis W. Murray, Senior Physical Scientist
The Rand Corporation, Santa Monica, California

*Material contained in this paper will be submitted for presentation before the AIAA 12th Aerospace Sciences Meeting, Fluid Dynamics Session, 30 January-1 February 1974.

INTRODUCTION

Analytical models for fires and their associated environment may be useful tools for predicting and studying the dynamics of flow surrounding a source of disturbance and for studying the production and distribution of pollutants that result from combustion, photochemical processes, etc. These models may also prove to be useful tools for long-range planning, forecasting, and management of the environment. It is emphasized that analytical and/or physical modeling is a difficult task. It will not serve as a substitute for good experimental measurements, but it is a prerequisite to good experimental planning. Physical models are readily employed in systems analysis to study the overall response to a specified perturbation, simultaneously taking into consideration the combined effects of many variables and parameters. The state of the art of fire and environmental flow dynamics is not satisfactorily developed at the present time. This is due to the lack of pertinent information that could be developed through numerical simulation, and also due to the lack of sufficient detailed observations in the field.

THE GENERAL MODEL

Flow field equations are presented as time-smoothed equations of change for an incompressible fluid, and subsequently reduced to simplified two-dimensional flows. The present state of the art allows these equations to be extended to the 2-D fire front as well as the axisymmetric fire plume. A quasi steady-state flow field results when the time derivative equals zero and does not appear in the general equations, but parameters and boundary conditions may be time-dependent.

The formulation will be focused on turbulent flows; however, the equations for laminar and turbulent flows can be reduced to one equivalent set of partial differential equations when the effective transport properties are employed [see reference (2)].

The macroscopic description of the state of a fluid system is defined by the number densities of the various chemical species, the mass average (or stream) velocity, and the temperature. These variables are related to quantities that are conserved in molecular collisions; i.e., the masses of individual molecules, the momentum, and the energies of colliding molecules. For each of these summational invariants there is an associated equation of change; i.e., the equations of continuity of individual species, the equation of motion, and the equation of energy balance. Global or overall continuity is also preserved. The general form of these equations as applicable to multicomponent and turbulent flow problems is as follows [see reference (3)]:

$$\frac{\partial C_A}{\partial t} = -\left[\frac{\partial}{\partial x}(v_x C_A) + \frac{\partial}{\partial y}(v_y C_A) + \frac{\partial}{\partial z}(v_z C_A)\right]$$

$$+ \mathcal{D}_{AX}\left[\frac{\partial^2 C_A}{\partial x^2} + \frac{\partial^2 C_A}{\partial y^2} + \frac{\partial^2 C_A}{\partial z^2}\right] - k_n''' C_A^{\,n} \qquad (1\text{-}1)$$

$\vdots$

$$\frac{\partial C_N}{\partial t} = -\left[\frac{\partial}{\partial x}(v_x C_N) + \frac{\partial}{\partial y}(v_y C_N) + \frac{\partial}{\partial z}(v_z C_N)\right] + \mathcal{D}_{NX}\left[\frac{\partial^2 C_N}{\partial x^2} + \frac{\partial^2 C_N}{\partial y^2} + \frac{\partial^2 C_N}{\partial z^2}\right] - k_n''' C_N^{\,n} \tag{1-2}$$

where C represents concentration; $\underset{\sim}{v} = (v_x, v_y, v_z)$ is velocity; $\mathcal{D}$ is the diffusion coefficient; X represents any species from A to N; and k''' is the reaction rate constant. For simplification, it will be assumed that k''' is independent of position and is a function of temperature only. The above equations are for the continuity of species A, B, ..., N, which are assumed to be generated and/or destroyed by an n-th order chemical reaction. In turbulent flows, C_A, C_B, ..., C_N will be rapidly oscillating functions of time. It is then convenient to replace these quantities by the sum of time-smoothed values $\overline{C_A}$, $\overline{C_B}$, ..., $\overline{C_N}$ and turbulent concentration fluctuations C_A', C_B', ..., C_N'. Thus

$$C_A = \overline{C_A} + C_A'$$

$$\vdots$$

$$C_N = \overline{C_N} + C_N'$$

Substituting $\overline{C_N} + C_N'$ and $\overline{v_i} + v_i'$ for C_N and v_i respectively, one obtains, after time averaging, the following forms of the continuity equation:

$$\frac{\partial \overline{C_N}}{\partial t} = -\left[\frac{\partial}{\partial x}(\overline{v_x}\ \overline{C_N}) + \frac{\partial}{\partial y}(\overline{v_y}\ \overline{C_N}) + \frac{\partial}{\partial z}(\overline{v_z}\ \overline{C_N})\right]$$

$$\underline{-\left[\frac{\partial}{\partial x}(\overline{v_x' C_N'}) + \frac{\partial}{\partial y}(\overline{v_y' C_N'}) + \frac{\partial}{\partial z}(\overline{v_z' C_N'})\right]}$$

$$+ \mathscr{D}_{NX}\left[\frac{\partial^2 \overline{C_N}}{\partial x^2} + \frac{\partial^2 \overline{C_N}}{\partial y^2} + \frac{\partial^2 \overline{C_N}}{\partial z^2}\right]$$

$$- \left\{\begin{matrix} k_1''' \overline{C_N} \\ \text{or} \\ k_2'''\left(\overline{C_N}^2 + \overline{C_N'^2}\right)\end{matrix}\right\} \qquad (1\text{-}3)$$

The underlined expressions represent additional terms due to time smoothing of the species continuity equation.

The time smoothed equation for continuity of the N-th species can be written in vector notation as

$$\frac{D\overline{C_N}}{Dt} = -(\nabla \cdot \overline{\underset{\sim}{J}}_N^{(\ell)}) - \underline{(\nabla \cdot \overline{\underset{\sim}{J}}_N^{(t)})} - \left\{\begin{matrix} k_1''' \overline{C_N} \\ \text{or} \\ k_2'''\left(\overline{C_N}^2 + \overline{C_N'^2}\right)\end{matrix}\right\} \qquad (1\text{-}4)$$

The symbol $\overline{\underset{\sim}{J}}$ is defined as $\overline{\underset{\sim}{J}} = -\mathscr{D}_{NX}\nabla\overline{C_N}$, and the $\frac{D}{DT}$ operator is defined as $\frac{D}{DT} = \frac{\partial}{\partial t} + \overline{\underset{\sim}{v}} \cdot \nabla$. The superscript (t) represents a time-smoothed value, and (ℓ) represents a departure from this value.

By similar considerations the time-smoothed equations of motion, energy transport, and global continuity, have been shown to be as follows [see Bird, et al., reference (1); also reference (3)]:

$$\rho \frac{D\bar{\underset{\sim}{v}}}{Dt} = -\nabla\bar{p} - \left[\nabla \cdot \bar{\tau}^{(\ell)}\right] - \left[\nabla \cdot \tilde{\tau}^{(t)}\right] + \rho\underset{\sim}{g} \quad (2\text{-}1)$$

$$\rho\hat{c}_p \frac{D\bar{T}}{Dt} = -(\nabla \cdot \bar{\underset{\sim}{q}}^{(\ell)}) - (\nabla \cdot \bar{\underset{\sim}{q}}^{(t)} + \mu\phi_v^{(\ell)} + \mu\phi_v^{(t)}) \quad (3\text{-}1)$$

$$(\nabla \cdot \bar{\underset{\sim}{v}}) = 0 \quad (4\text{-}1)$$

In the above equations, $\bar{\tau}^{(\ell)}$ and $\bar{\tau}^{(t)}$ are the Reynolds stress tensors; $\bar{\underset{\sim}{q}}^{(\ell)}$ and $\bar{\underset{\sim}{q}}^{(t)}$ are equal to $-k\nabla\bar{T}$ and $-k\nabla T'$ respectively, where k is coefficient of thermal conductivity; $\underset{\sim}{q} = \bar{\underset{\sim}{q}}^{(\ell)} + \bar{\underset{\sim}{q}}^{(t)}$; and $\phi_v^{(\ell)}$ and $\phi_v^{(t)}$ represent expressions for the viscous dissipation function and the time-smoothed dissipation function respectively.

The above set of equations is satisfactory for specifying the composition and state variables in turbulent reactive flows. This set of equations constitutes a basic physical model suitable for describing the turbulent flow fields surrounding a source such as fire and associated environment. However, it is highly probable that radiation is an important mechanism of heat transfer, and accordingly, a model for radiation is desirable.

The heat transfer due to radiation can be accounted for as follows [reference (4)]:

$$\left(\frac{\partial}{\partial r} q_r\right) = R - A \quad (5\text{-}1)$$

where R is the rate of radiant emission per unit volume, A is the rate of energy absorption per unit volume, and r is the generalized coordinate. For a given system one can define an absorption coefficient μ_ν with dimension L^2M^{-1} for radiation of frequency ν. If $R_\nu(r)$ is the energy emitted per unit volume per unit time in unit frequency range ν, and $q_\nu(r)$ is the radiation energy flux in this frequency range, then

$$R(r) = \int_0^\infty R_\nu(r)\ d\nu \tag{6-1}$$

$$q_\nu(r) = \int_0^\infty R_\nu(r) \left(\frac{r_{12} - r}{r_{12}}\right) \frac{1}{4r_{12}^2} \exp\left[-\int_0^{r_{12}} \rho\mu_\nu\ d\ell\right] dr_{12} \tag{7-1}$$

Equation (6-1) can be integrated for two special cases: opaque materials (flame fronts with large amounts of smoke), in which absorption or radiation is so intense that the radiation is in local thermodynamic equilibrium; and transparent materials, in which there is little self-absorption of radiation. If the absorption coefficient can be taken as constant,

$$q_r = \frac{c}{3}\left[\int_0^\infty \frac{1}{\rho\mu_\nu} \frac{d}{dT}\left(\frac{8\pi h\nu^3}{c^3} \frac{1}{(\exp\ [h\nu/kT] - 1)}\right) d\nu\ \frac{\partial T}{\partial r}\right] \tag{8-1}$$

For weak absorption in non-luminous flame, Eq. (7-1) may be integrated in polar spherical coordinates to give

$$q = \frac{ce_\nu}{4}\left(1 - \exp\ [-\rho\mu_\nu]L\right) \tag{9-1}$$

The total axial component of radiative flux is then

$$q_R = \int_0^{\infty} q_\nu \, d\nu = \frac{\varepsilon\sigma T^4}{4}\left[1 - \frac{1}{(\sigma T^4)}\int_0^{\infty} e_\nu \exp(-\rho\mu_\nu)L \, d\nu\right] \qquad (10\text{-}1)$$

where the factor $\varepsilon\sigma T^4$ represents the black body radiation at temperature T, and terms enclosed in brackets are the effective emissivity of the fluid, $\varepsilon(T, \rho L)$. Thus, in order to evaluate Eq. (10-1), experimental measurements of $\varepsilon(T,\rho L)$ as a function of T and ρL for the fire environment must be made.

Another radiative transfer problem that appears to be applicable in systems analysis of fires is that of the "stationary radiation front." If conditions permit, the temperature vs. x (the horizontal coordinate) can be related. The simple geometry of an infinite flat plane with a moving fire front of velocity v_x at t_o and a constant specific heat $\hat{c}_v$ is considered. The kinetic energy and thermal conductivity of the fluid are neglected, and external forces are assumed to be zero. The absorption is assumed to be so intense that the radiation flux can be expressed in terms of the Rosseland mean free path as

$$\rho v_x \hat{c}_v (T - T_\infty) = q_{Rx} - (q_{Rx})_\infty \qquad (11\text{-}1)$$

It is assumed that T_∞ and $(q_{Rx})_\infty$ are much smaller than the corresponding values at the fire front. For the above assumptions, the energy balance for the steady state can be represented as

$$\rho v_x \hat{c}_v T - \frac{\hat{c}_v \lambda_R}{3} \frac{d(\sigma T^4)}{dT} \frac{dT}{dx} \qquad (12\text{-}1)$$

Differentiation of (11-1) yields $\frac{dT}{dx}$ for use in (12-1).

The mean free path is assumed to vary as the s power of temperature; i.e., $\lambda_R = \lambda_0 T^s$.

A solution of Eq. (12-1) is the following [see reference (4)]:

$$(T^{s+3} - T_0^{s+3}) - \frac{3(s + 3)}{4} \frac{\rho \hat{c}_v v_x x}{\lambda_0 c \sigma} = 0 \qquad (13-1)$$

For

$$x_0 = \frac{4\lambda_0 c \sigma T_0^{s+3}}{3(s + 3)\rho \hat{c}_v u},$$

$$T = T_0 (1 - \frac{x}{x_0})^{1/(s+3)} \qquad (14-1)$$

The above account of radiation in a fire environment is perhaps overly simplified. However, a solution to the integro-differential equation for radiation transfer is not practical at this time.

THE THERMAL CONVECTION MODEL

For the work reported herein, a model for convection was used that ignores radiative transfer and treats a fluid consisting only of air, water vapor, and condensed drops. In this model the dynamics is emphasized rather than the chemistry. Cloud microphysics is treated parametrically rather than explicitly.

Thermal convection on the scale of a fire situation was simulated by numerical solution of the Boussinesq equations of motion, the first law of thermodynamics, and the equations of continuity for air and water substance. The Boussinesq approximation describes a fluid that is incompressible but not hydrostatic. Hence, a stream function ψ can be defined such that the horizontal and vertical components of the wind are

$$v_x = -\frac{\partial\psi}{\partial z} \qquad v_z = \frac{\partial\psi}{\partial x} \tag{15-1}$$

in two-dimensional flow in Cartesian (x,y,z) coordinates, and

$$v_r = -\frac{1}{r}\frac{\partial\psi}{\partial z} \qquad v_z = \frac{1}{r}\frac{\partial\psi}{\partial r} \tag{16-1}$$

in axially symmetric flow in cylindrical (r,θ,z) coordinates.

A vorticity equation derived from the equation of motion is used to compute the changes in ψ and consequently in the components of $\underset{\sim}{v}$. Concurrently, the first law of thermodynamics, the equation of continuity for water substance, and a parameterization of the microphysics of condensation and evaporation are used to determine changes in temperature departure and moisture content; hence in buoyancy.

This model is based on that developed by Murray, et al. (5,6,7) to simulate cumulus convection and bears some similarity to the cumulus model of Orville (8). The boundary conditions require that the normal component of wind at the lower, outer, and upper boundaries vanish. The outer and upper boundaries are chosen at a distance from the disturbed region sufficient to minimize unwanted interactions. In addition, the horizontal component of wind and the horizontal derivative of the vertical component of wind are taken to be zero at the axis of symmetry. Eddy diffusion of the Fickian type is included in the equations. It has been found in the present instance that eddy-diffusion coefficients of 200, 40, and 500 m^2 sec^{-1} for momentum, moisture, and temperature respectively lead to values of those properties that are of the order of magnitude of observed values.

In the present experiment the rectilinear geometry was used, and the convection was driven by a time-dependent temperature distribution specified at the earth's surface. This forcing function was based on observations of a typical forest fire (9); it is illustrated in Fig. 1.

The computed wind fields at one, two, four, and six minutes of simulated time are shown in Figs. 2-5. The arrows fly with the wind, and each half barb represents a speed of 5 m sec^{-1}, each full barb 10 m sec^{-1}, and each pennant 50 m sec^{-1}. The direction and speed are also given by the digits near the heads of the arrows. The first two digits (or one digit with the leading zero dropped) show the direction in tens of degrees from which the wind is blowing, measured clockwise from the "12 o'clock" position. The last two numbers give the speed in m sec^{-1}. The values shown are found to be in agreement with observations.

The departures of temperature (°C) from the initial value are contoured in Figs. 6-10. The occasional crossed contours were introduced by interpolation made by the automatic contouring program. It will be noted that by 6 minutes, the excess of temperature in the core of the fire is greater than 100°C. Unfortunately, there appears to be little experimental data available on temperature departures in the vicinity of large fires, and consequently it is difficult to relate the simulated results to reliable measurements.

In its present state of development, the program can handle two geometries: cylindrical coordinates with axial symmetry and Cartesian coordinates with symmetry about the Y-Z plane. The version in cylindrical coordinates cannot realistically simulate ambient winds, but can only simulate an isolated fire under calm conditions. It is capable of portraying the low-level indraft, the high-level outdraft, the central updraft, and the surrounding subsidence.

The version in Cartesian coordinates has the disadvantage of producing downdrafts that are somewhat stronger than those observed. Moreover, with the symmetry condition imposed, it can handle ambient winds no better than the version in cylindrical coordinates. However, it should be an easy matter to remove the symmetry condition, whereupon the Cartesian version could readily take care of an ambient wind with or without vertical shear, not to mention a non-level lower boundary. Thus it would be suitable for modeling a firefront.

Still other modifications to increase the utility of this program for simulating the dynamics of a real fire and its associated environment are needed and feasible. Besides those already mentioned, the provision for modeling fire spread by winds and firebrands and the provision for modeling the spread of noxious gases come readily to mind.

The model is sufficiently general and flexible that all of these improvements, and others as well, can readily be incorporated. The greatest difficulty foreseen is overcoming the numerical instability that results from the strong temperature gradients in a fire. It appears, however, that with a fine mesh, sufficiently short time step, and careful choice of numerical techniques, this problem can be overcome. With the model further developed as described above, numerical simulation of fires and their associated environments for more realistic conditions holds promise of becoming a useful analytic tool.

REFERENCES

1. Bird, R. B., W. E. Stewart, and E. N. Lightfoot, 1966: *Transport Phenomena*. New York: John Wiley and Sons, Inc., 780 pp.

2. North American Rockwell Company, 1969: *Application of Aerospace Technology to the Simulation of Mass Fire Behavior*, SID69-389, 75 pp.

3. Corrsin, S., 1958: "Statistical Behavior of a Reacting Mixture in Isotropic Turbulence," *Physics of Fluids*, Vol. 1, No. 1, pp. 42-47.

4. Hirschfelder, J. O., O. F. Curtiss, and R. B. Bird, 1954: *Molecular Theory of Gases and Liquids*. New York: John Wiley and Sons, Inc., 1219 pp.

5. Murray, F. W., and C. E. Anderson, 1965: *Numerical Simulation of the Evolution of Cumulus Towers*, Report SM-49230, Douglas Aircraft Co., 97 pp.

6. Murray, F. W., 1970: "Numerical Models of a Tropical Cumulus Cloud with Bilateral and Axial Symmetry," *Monthly Weather Review*, Vol. 98, No. 1, pp. 14-28.

7. Murray, F. W., and L. R. Koenig, 1972: "Numerical Experiments on the Relation Between Microphysics and Dynamics in Cumulus Convection," *Monthly Weather Review*, Vol. 100, No. 10, pp. 717-731.

8. Orville, H. D., 1965: "A Numerical Study of the Initiation of Cumulus Clouds over Mountainous Terrain," *Journal of the Atmospheric Sciences*, Vol. 22, No. 6, pp. 684-699.

9. Countryman, Clive M., 1969: *Project Flambeau--An Investigation of Mass Fire (1964-1967)*, Final Report, Vol. 1, prepared for Office of Civil Defense, Office of the Secretary of the Army, Washington, D. C. 20310, under OCD Work Order No. OCD-PS-65-26. Work Unit 2536A.

Fig. 1- FORCING FUNCTION EMPLOYED TO CAUSE NUMERICAL SIMULATION
OF FIRE TO PROCEED - TEMPERATURE TAKEN AT EARTH'S SURFACE
(Ignition was simultaneous over entire radial area of fire)

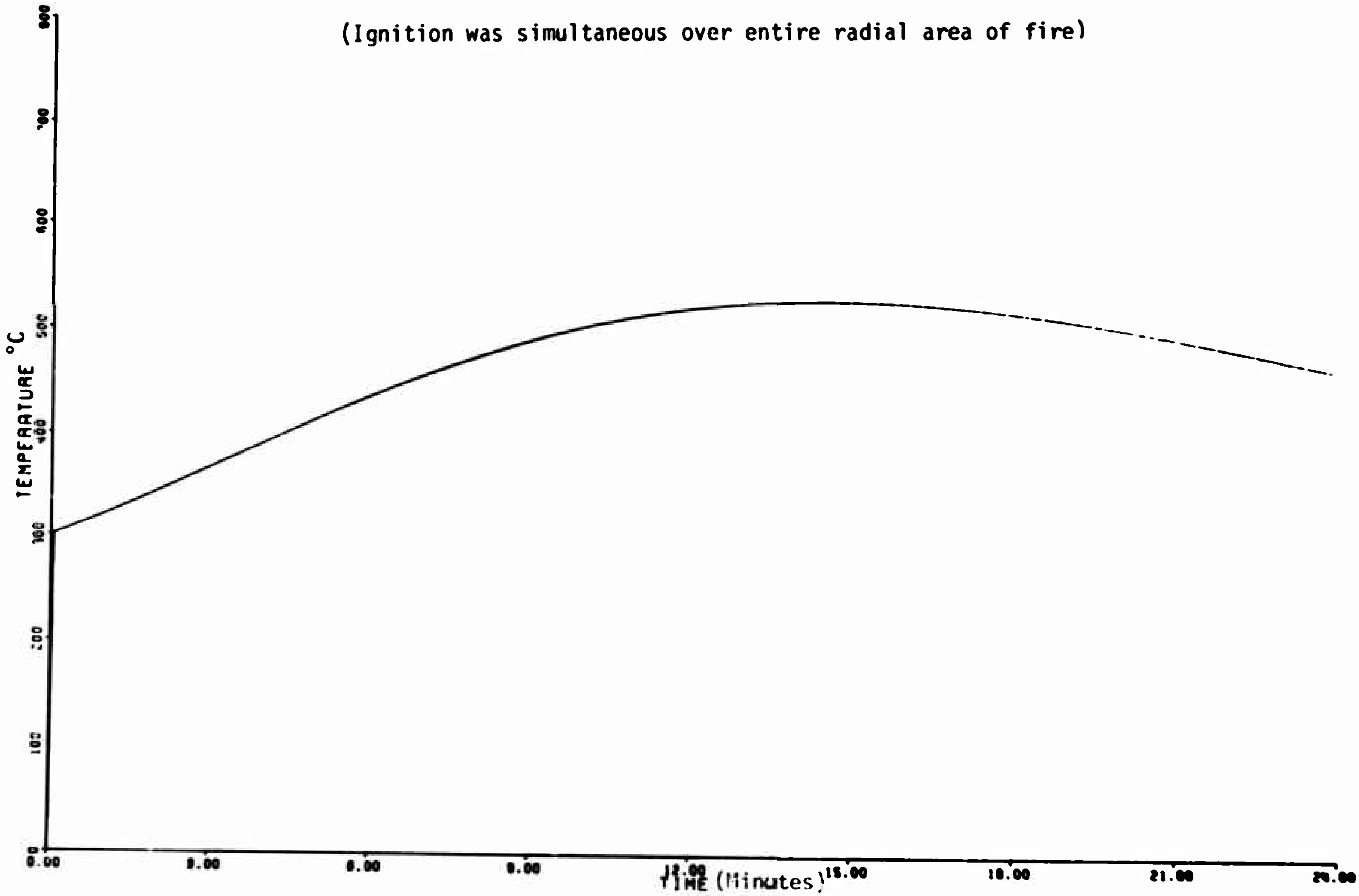

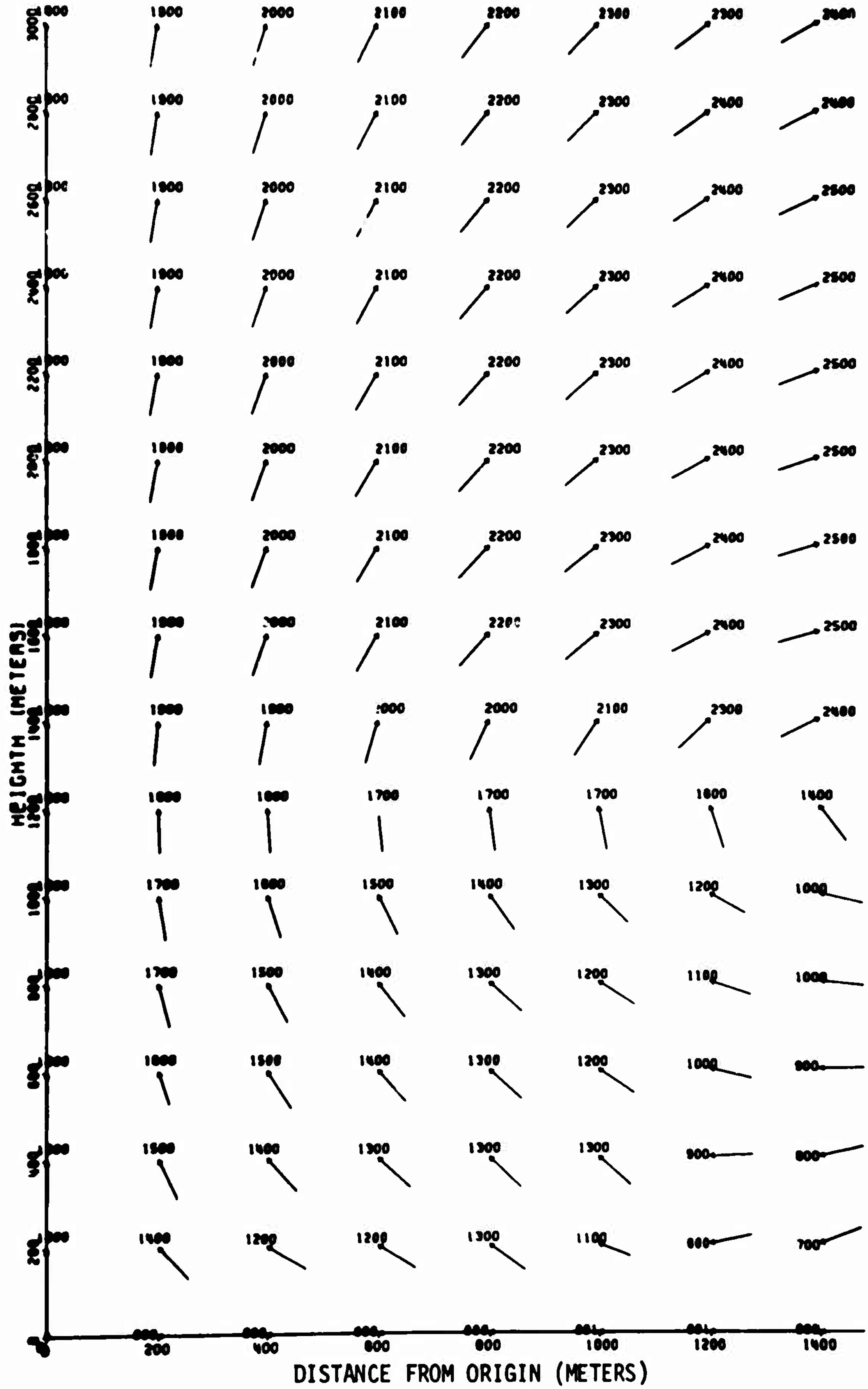

Fig. 2--Wind field at 1 min of simulated time.

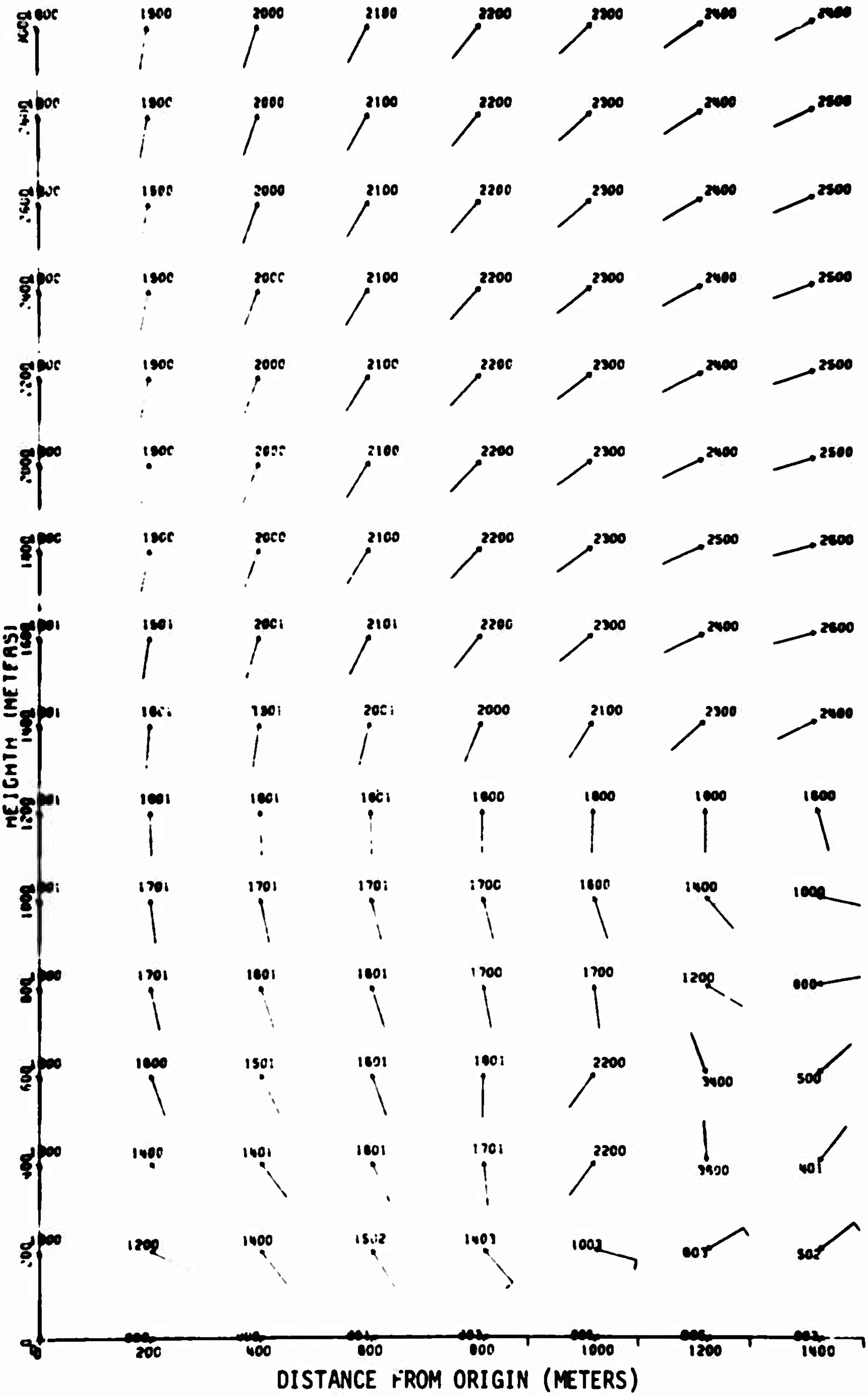

Fig. 3--Wind field at 2 min of simulated time.

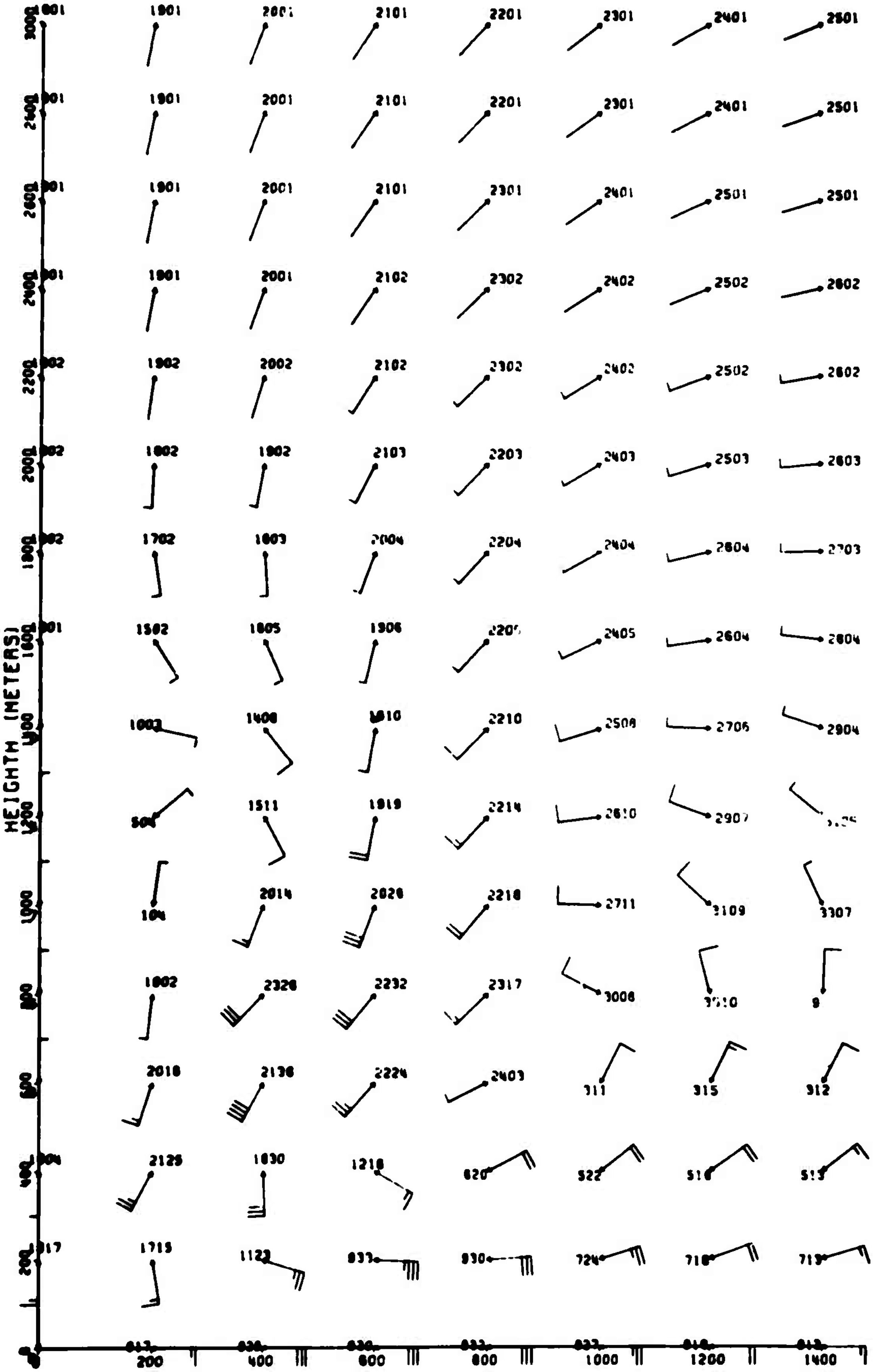

Fig. 4--Wind field at 4 min of simulated time.

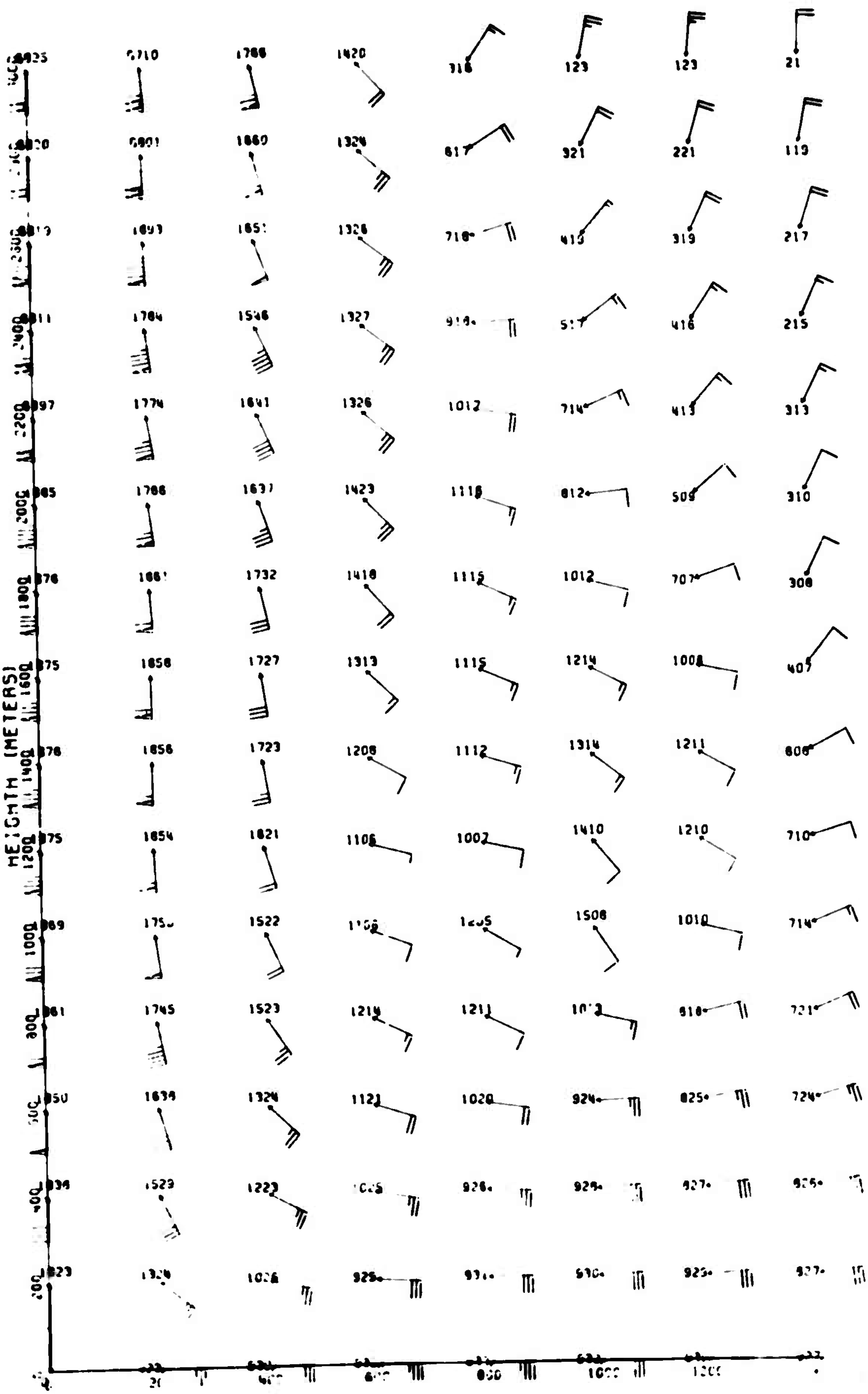

DISTANCE FROM ORIGIN (METERS)

Fig. 5--Wind field at 6 min of simulated time.

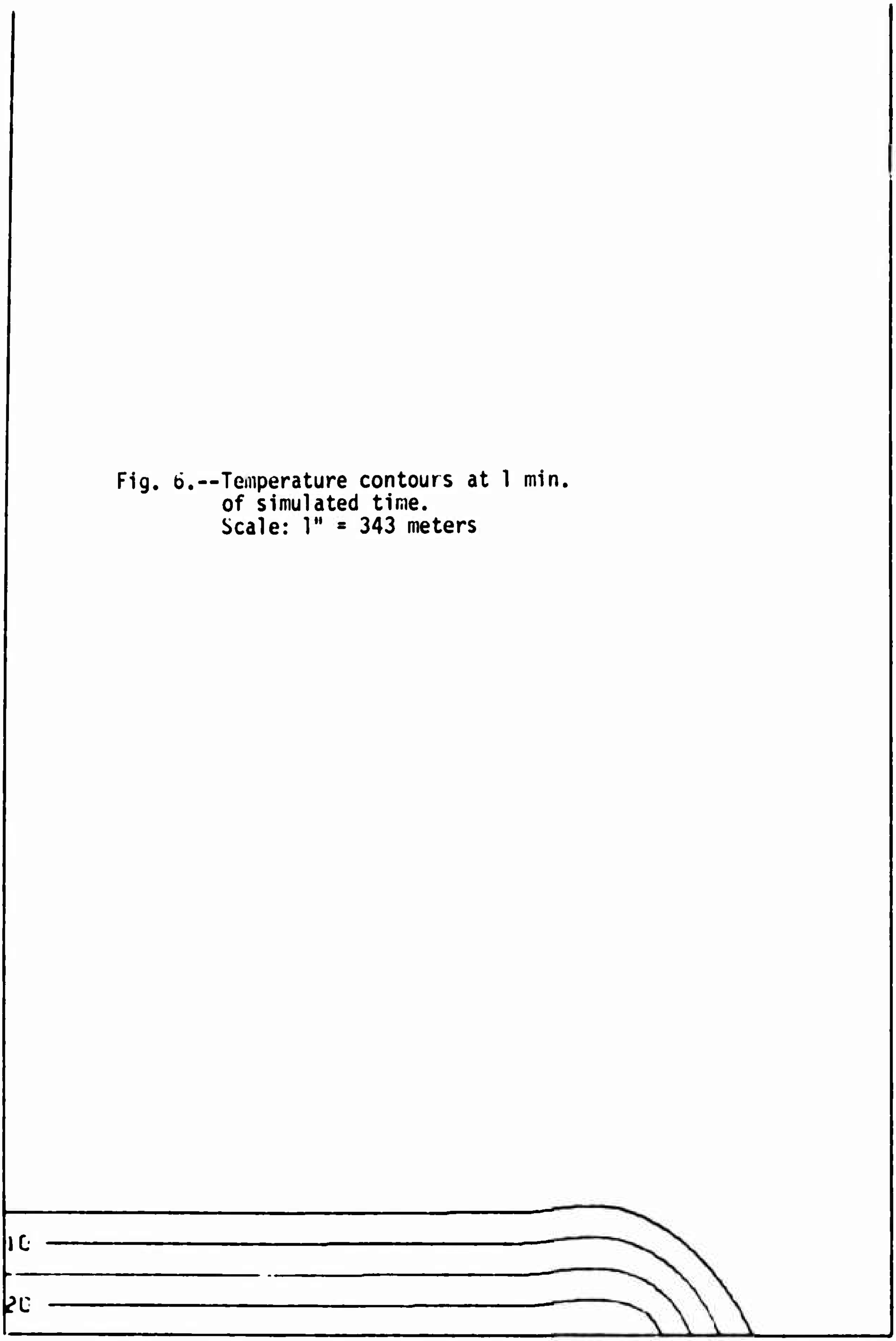

Fig. 6.--Temperature contours at 1 min.
of simulated time.
Scale: 1" = 343 meters

Fig. 7.--Temperature contours at 2 min.
simulated time
Scale: 1" = 343 meters

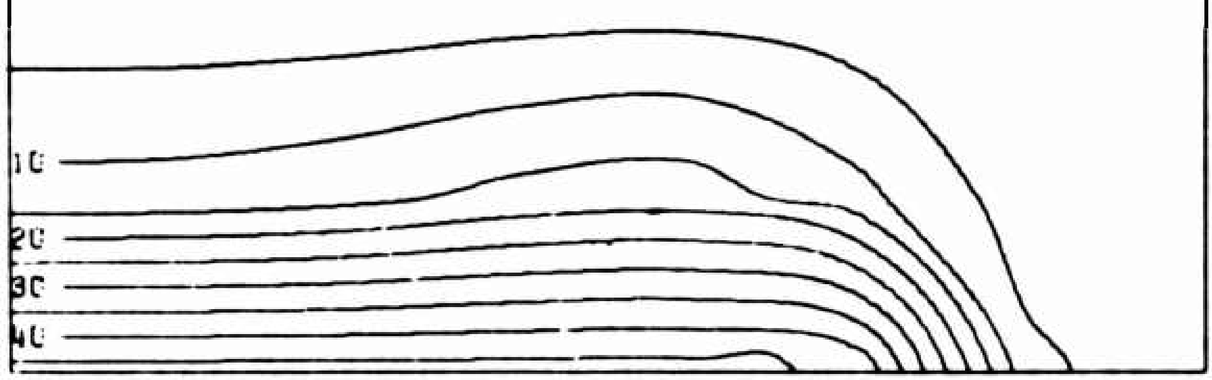

Fig. 8.--Temperature contours at 3 min.
simulated time.
1" = 343 meters

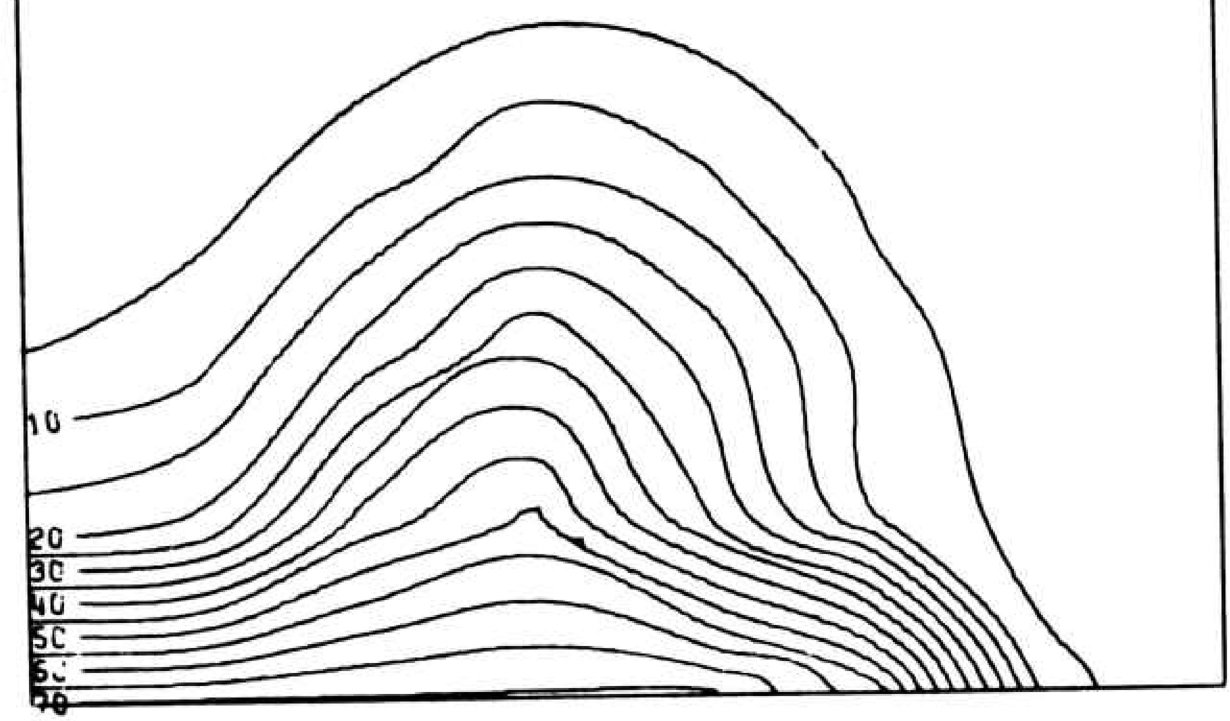

Fig. 9.--Temperature contours at 4 min.
of simulated time.
1" = 343 meters

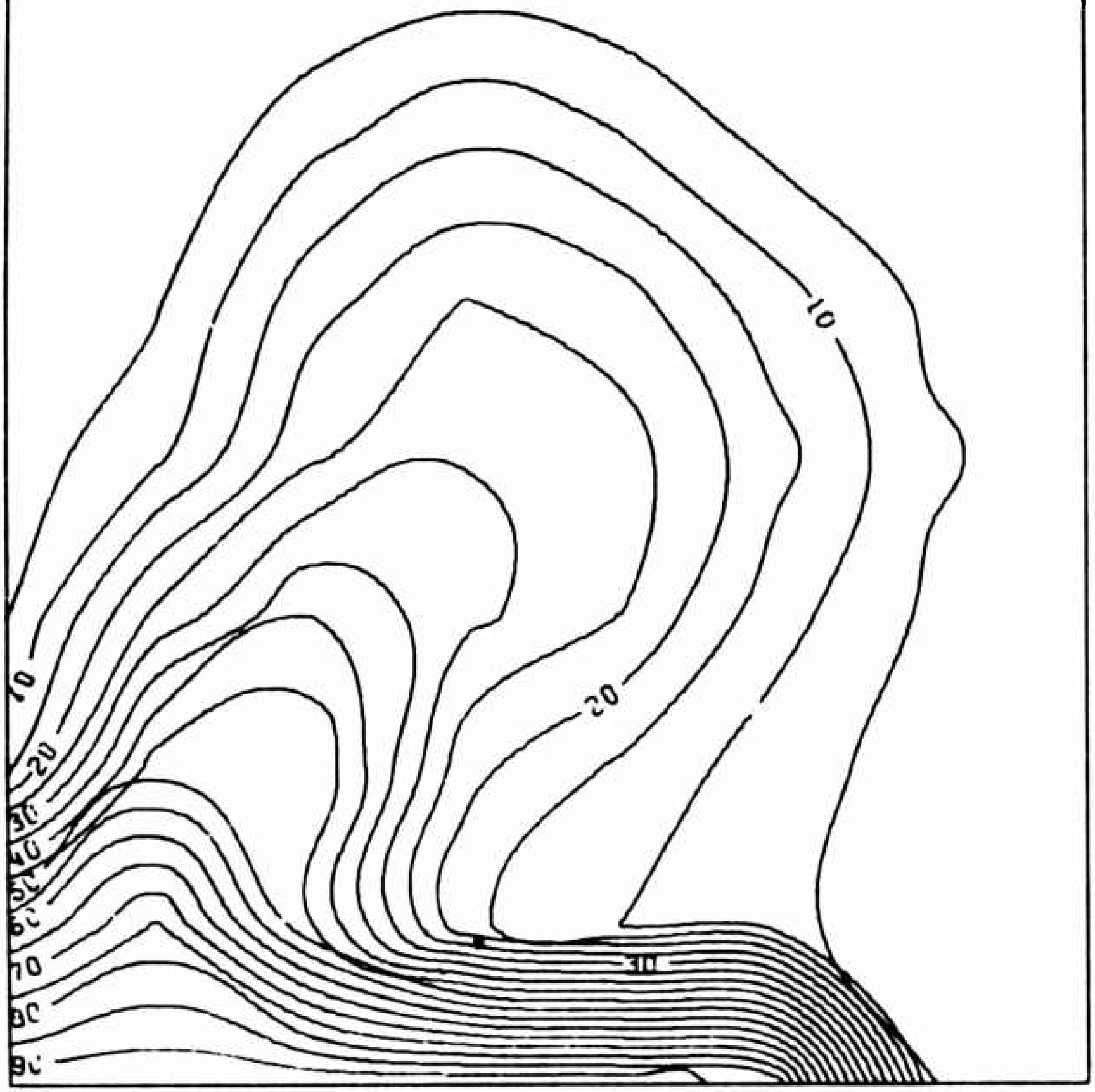

Fig. 10.--Temperature contours at 6 min.
of simulated time.
Scale: 1" = 343 meters